

Restructuring Tungsten Thin Films into Nanowires and Hollow Square Cross-Section Microducts

Prahalad M. Parthangal^{1,2}, Richard E. Cavicchi², Christopher B. Montgomery², Shirley Turner² and Michael R. Zachariah^{1,2,*}

University of Maryland¹, College Park, MD 20742, and National Institute of Standards and Technology², Gaithersburg, MD 20899

* Corresponding author (mrz@umd.edu)

Keywords: Tungsten oxide nanowires, Hollow square microducts, Chemical sensor

We report on the growth of nanowires and unusual hollow microducts of tungsten oxide by thermal treatment of tungsten films in a RF H₂/Ar plasma at temperatures between 550-620 °C. Nanowires with diameters of 10-30 nm and lengths between 50-300 nm were formed directly from the tungsten film, while under certain specific operating conditions hollow microducts having edge lengths $\sim 0.5 \mu\text{m}$ and lengths between 10-200 μm were observed. Presence of a reducing gas such as H₂ was crucial in growing these nanostructures as was trace quantities of oxygen necessary to form a volatile tungsten species. Preferential restructuring of the film surface into nanowires or microducts appeared to be significantly influenced by the rate of mass-transfer of gas phase species to the surface. Nanowires were also observed to grown on tungsten wires under similar condition. A surface containing nanowires, annealed at 500 °C in air, exhibited capability of sensing trace quantities of nitrous oxides (NO_x).

Growth of nanostructures like nanowires,^{1,2} nanotubes,^{3,4} nanobelts⁵ etc. has attracted tremendous research interest recently. Due to their almost one-dimensional structure, they possess unique electrical, thermal, optical and mechanical properties, which may be exploited in a variety of applications. Advances in the growth of such high aspect ratio structures have been hampered by difficulties in growing them with controllable dimensions, morphology, and phase purity. The most common techniques to fabricate these nanostructures include e-beam lithography,⁶ solution phase synthesis,⁷ vapor phase evaporation/condensation,⁸ and template-directed synthesis.^{9,10} In the case of nanowires, transition metals like tungsten could find applications in electronic devices, sensors, and magnetic recording devices.^{11,12}

Very recently, Lee et al.¹³ reported the growth of tungsten nanowires of less than 100 nm in diameter and about 1 μm in length by thermal treatment of tungsten films in the presence of H_2 , and demonstrated excellent field emission properties. Gu et al.¹⁴ grew tungsten oxide nanowires on metal tungsten tips (prepared by electrochemical etching of tungsten wires) heated in argon. They observed tungsten oxide nanowires between 10-30 nm in diameter and about 300 nm in length. Well-aligned nanowire arrays of molybdenum oxide were grown through thermal evaporation at 1100 $^{\circ}\text{C}$ by Zhou et al.,¹⁵ and subsequently reduced to molybdenum nanowires under a heated H_2 atmosphere. Using a similar approach, Liu et al.¹⁶ synthesized large-scale arrays of aligned tungsten oxide nanorods by heating a spiral tungsten coil to ~ 1000 $^{\circ}\text{C}$. Vaddiraju et al.¹⁷ also demonstrated vapor phase synthesis of tungsten and tungsten oxide nanowires in a hot-filament CVD reactor, at temperatures above the decomposition temperature of tungsten oxide (~ 1450 $^{\circ}\text{C}$). Apart from nanowires, other nanostructures like whiskers and hollow fibers of tungsten oxide have been studied in the past.¹⁸⁻²¹ More recently, Li et al.²² grew $\text{W}_{18}\text{O}_{49}$ nanotubes and nanowires by infrared irradiation on W foils under different vacuum conditions.

In this work, we show how an RF H_2/Ar plasma can be used to substantially reduce the processing temperature required to restructure tungsten thin films into tungsten oxide nanowires. We also show a mode that we observe in regions of restricted gas-phase mass transfer in which the tungsten film is converted into novel hollow microducts of square cross-section. These microducts can be quite long 10-200 μm with edge lengths of 0.5 μm . We also discuss the difference in growth mechanisms between nanowires and microducts, the former occurring by nucleation from the vapor phase, and the latter involving surface restructuring of the thin film, and growth in regions of restricted gas-phase mass transfer. Finally, we present the gas sensing capabilities of the nanowires annealed in air.

Tungsten films of 300-350 nm were deposited on a flat, polished substrate (1 cm x 1 cm) of sapphire by DC-magnetron sputtering from a high purity tungsten (99.99% pure) target with pure argon (99.9995% pure) as the sputtering gas. The substrate was then secured to a heater-plate assembly using a ceramic clip and transferred (in air) to a low-pressure CVD chamber where argon and H_2 were metered with mass flow controllers, and chamber pressure maintained at 5 torr during growth using a rotary mechanical rough pump. Ar flow rate was kept constant at 300 sccm for all experiments. The substrate temperature was then increased to 500-700 $^{\circ}\text{C}$ and monitored using a thermocouple in contact with the substrate. An RF-plasma was easily generated within the chamber by winding a copper coil around the 7.5 cm cylindrical quartz chamber, and the plasma power (20 W) was controlled using a matching network. Growth times were typically 10 minutes, after which the heater was turned off and the substrate was cooled to room temperature, while the chamber was continuously purged with Ar and H_2 . The morphologies of all films were observed using a Hitachi S-4000 field emission scanning electron

microscope (SEM).

Initially, experiments were conducted in the absence of the RF plasma. Heating the film in pure Ar to 750-800 °C without any H₂, resulted in the restructuring of the smooth tungsten surface into a grainy, nodular one, as seen in Figure 1a. However, when H₂ was introduced (30 sccm) along with Ar at these temperatures, nanowires appeared on the surface, similar to those observed by Lee et al.¹³ With an RF plasma, it was found that a lower substrate temperature and a lower concentration of H₂ also produced nanowires. Figure 1b shows the result of heating a tungsten film to ~ 550 °C with a reduced H₂ flow rate of 5 sccm for 10 minutes. A uniformly dense network of nanowires were seen to have grown with diameters between 10-30 nm and lengths between 0.5-1 μm. Increasing the substrate temperature to 600 °C as shown in Figure 1c, produced several larger tungsten crystallite structures in addition to nanowires. However above ~ 620 °C, no evidence of wires could be found; rather the films consisted of large crystallite structures of various shapes as well as solid square nanorods as seen in Figure 1d.

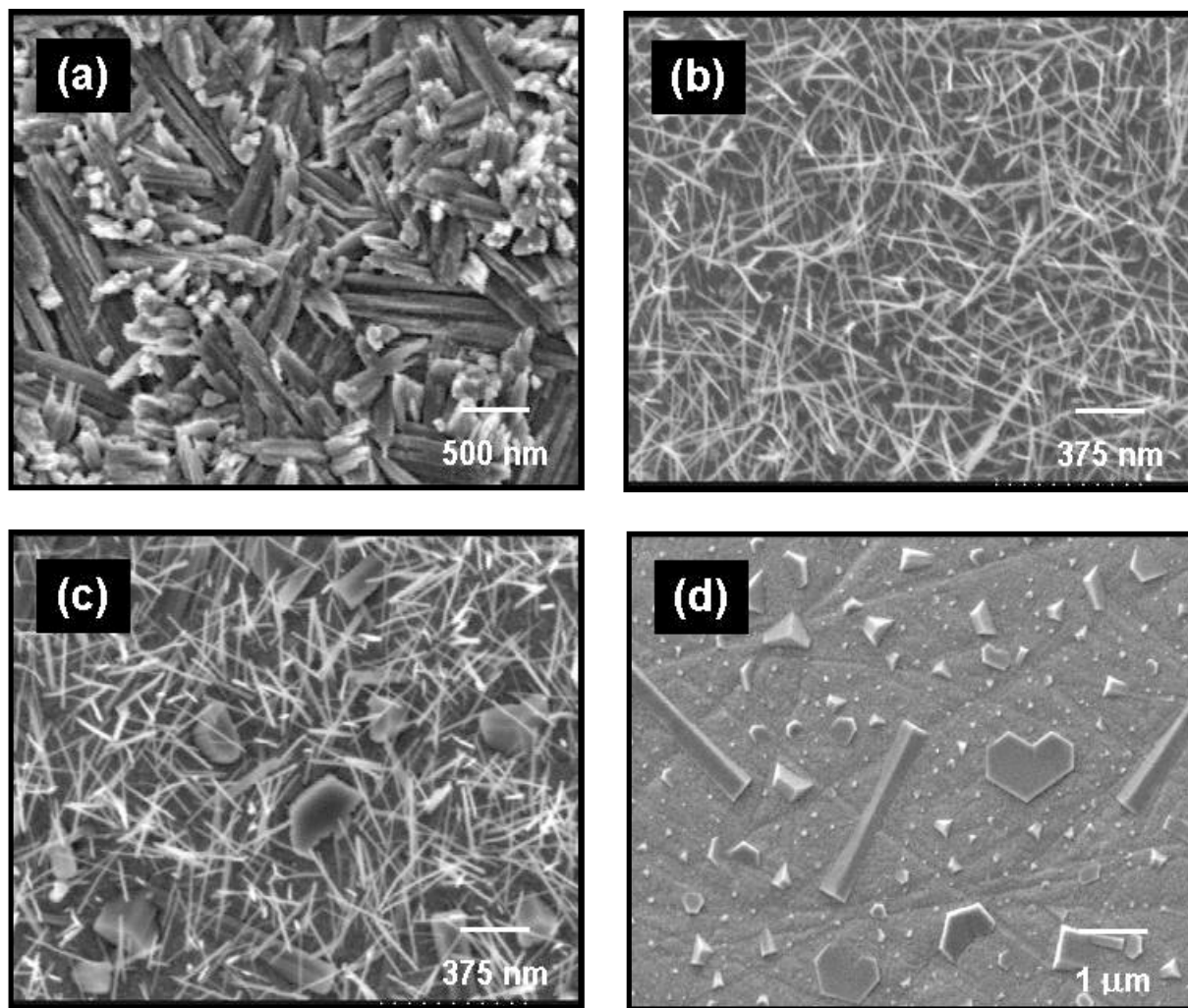


Figure 1. Micrographs of tungsten film surface – (a) heated in the absence of H₂, (b) nanowires, (c) nanowires

and crystallite structures, (d) crystallite structures and solid square nanorods.

A significant finding was that for samples which were heated to temperatures between 550-620 °C, several unusual hollow microstructures with a square cross-section (henceforth referred to as “microduct”) had grown in the region of the substrate underneath the ceramic clip that was securing the sample. These microducts had average edge lengths of $\sim 0.5\ \mu\text{m}$, wall thickness of about 20-30 nm, and lengths ranging from tens to a few hundreds of μm 's. The SEM images of the microducts are presented in Figure 2. To test the generality of the process, we heated a 0.005” diameter tungsten wire (Alfa Aesar), as well as a tungsten coated TEM grid (Pacific Grid Tech – 200 mesh) to 700 °C in Ar/H₂ within the chamber, and observed that nanowires grew over the entire surface of both the wire and the TEM grid (Figure 3).

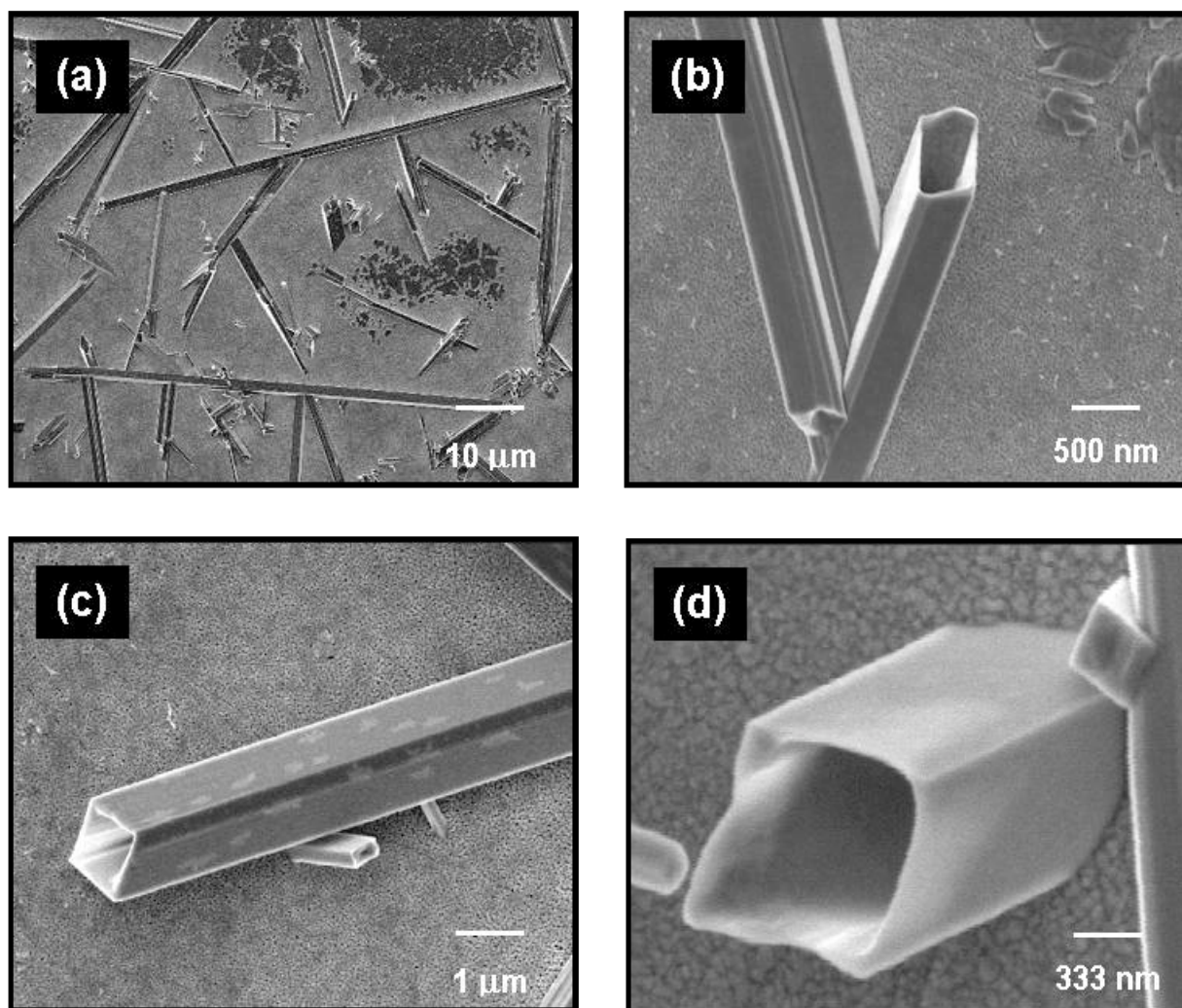


Figure 2. Micrographs of hollow microducts grown from the tungsten film, at different magnifications.

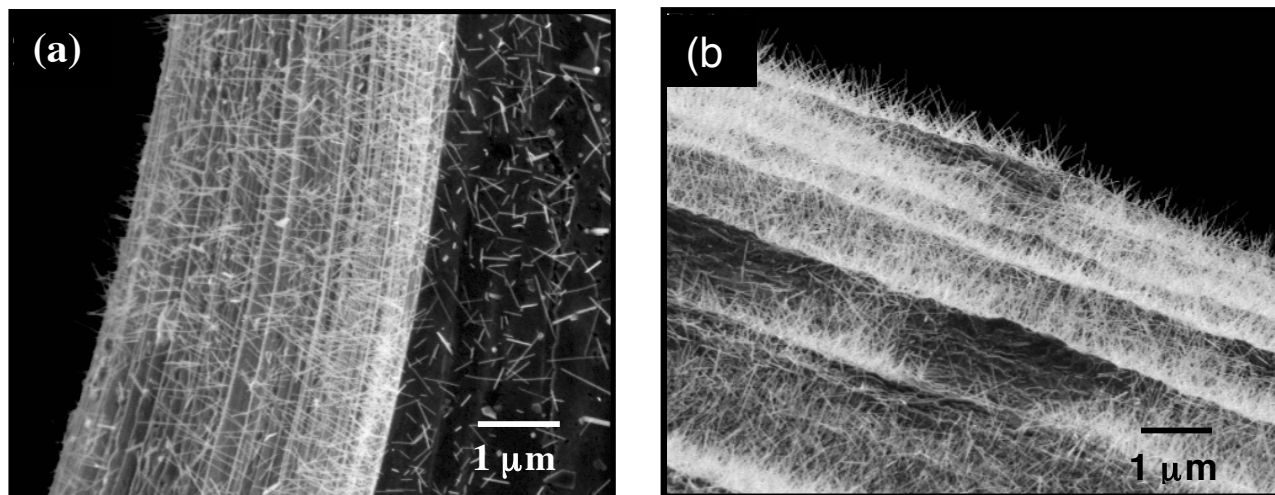


Figure 3. Micrograph of nanowires grown on a commercial tungsten TEM grid and a commercial tungsten wire.

Nanowires grown on the tungsten TEM grid were analyzed by high-resolution transmission electron microscopy (HRTEM) to obtain phase information and growth direction. A HRTEM image of a nanowire and electron diffraction patterns obtained from two different nanowires, are shown in Figure 4.

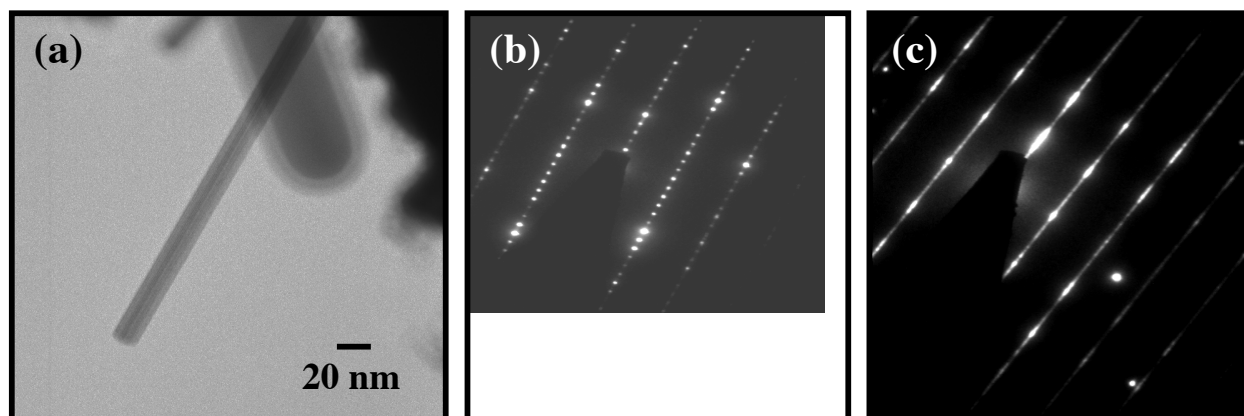


Figure 4. (a) HRTEM image of a nanowire. (b) & (c) Electron diffraction patterns obtained from two different nanowires.

Upon inspecting several different nanowires, two different electron diffraction patterns were obtained, as seen in Figures 4b and 4c. The d-spacings of 3.8 \AA and 17.5 \AA corresponding to the regularly spaced pattern, were observed to be closest to the d-spacing of $\text{W}_{18}\text{O}_{49}$. The streaked pattern obtained from some other nanowires, indicates the presence of disordered intergrowths which may be due to varying

oxygen stoichiometry in different nanowires. A further investigation will be required to explain the reasons for the occurrence of such different patterns from nanowires on the same sample.

Because no catalyst material was present to initiate the growth of nanowires, the VLS (vapor-liquid-solid) growth mechanism does not apply here. Growth of nanowires may be explained based on a modified VS (vapor-solid) mechanism, where the tungsten film deposited on the substrate acts as a self-catalytic layer. Upon heating the film to 550 °C in a low-pressure plasma (~ 4 torr), the volatile surface oxide evaporates. This vapor phase oxide should be reduced in the H₂ plasma to a lower tungsten oxide, which then re-condenses back on the film surface as a nanowire. The vapor phase mechanism was confirmed, as nanowires were also seen to form on a pristine silicon wafer placed just above the heated tungsten sample. This mechanism implied that a source of oxygen (background from the rough vacuum pumped chamber) played a necessary role in constantly oxidizing the tungsten film so as to create a volatile tungsten containing species. To test this hypothesis, we conducted experiments in a high vacuum chamber. A tungsten sample heated to about 700 °C in pure H₂ and Ar failed to produce any nanowires. However, when a trace amount of air or oxygen (1-2 vol. %) was bled into the system, nanowires appeared.

We believe that gas phase mass transfer rate of the reducing agent may play a pivotal role in determining whether growth of nanowires or microducts are preferred, since the latter grew only in specific regions underneath the clip. To test this hypothesis, we placed a ceramic substrate at a slight angle to the heated tungsten substrate as schematically illustrated in Figure 5. The purpose was to impose a mass transfer resistance of varying degree to the substrate and observe the resulting morphologies at different points along the length of the substrate. We discovered that the tungsten oxide nanowires grew over most of the sample, but with a higher density in the regions farthest from the contact point between the two substrates (Figure 5 – region 1). Microducts and tungsten oxide crystallite structures were observed to grow exclusively in the region where the gap between the substrate and sample was narrow (Figure 5 – region 2). The occurrence of nanowires with varying oxygen levels may also be explained through such an argument.

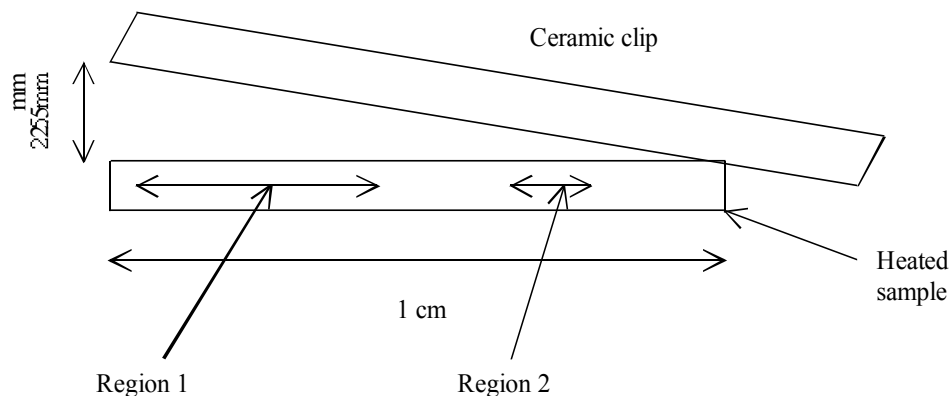


Figure 5. Schematic of sample-clip assembly – region 1 was covered with nanowires while region 2 contained microducts in addition to crystallite structures.

Mayers and Xia²³ recently reported on the growth of hollow nanotubes as well as solid nanorods of tellurium through a solution phase approach. They observed that varying the mass transfer rate of tellurium to the seed surface could control the type of nanostructure grown, a lower tellurium concentration resulting in the hollow nanotubes while a higher concentration resulted in solid nanorods. We believe that the hollow microducts of tungsten oxide grew only in regions on the substrate that offered maximum resistance to gas phase mass transfer of H_2 , which in turn influenced the rate of addition of tungsten oxide to the surface. At temperatures greater than 620 °C, the production rate of tungsten oxide atoms is enhanced allowing uniform addition of tungsten oxide over the entire surface and resulting in solid nanorods and other stable crystallite structures.

To verify the role of H_2 as reducing agent rather than as an agent for creation of a WH_x species, we replaced the H_2 with carbon monoxide (CO), and heated the sample to 550 °C in the RF plasma. The results were quite definitive in showing that H_2 was not necessary for the growth of nanowires so long as another reducing agent was present, as observed in Figure 6a. However, instead of hollow microducts with regular square cross-section, we observed several hollow nanostructures of irregular shapes (Figure 6b). This difference in nanostructures resulting from a different reducing agent may be due to the weaker reducing effect of CO in comparison to H_2 in addition to dissimilar mass transfer rates.

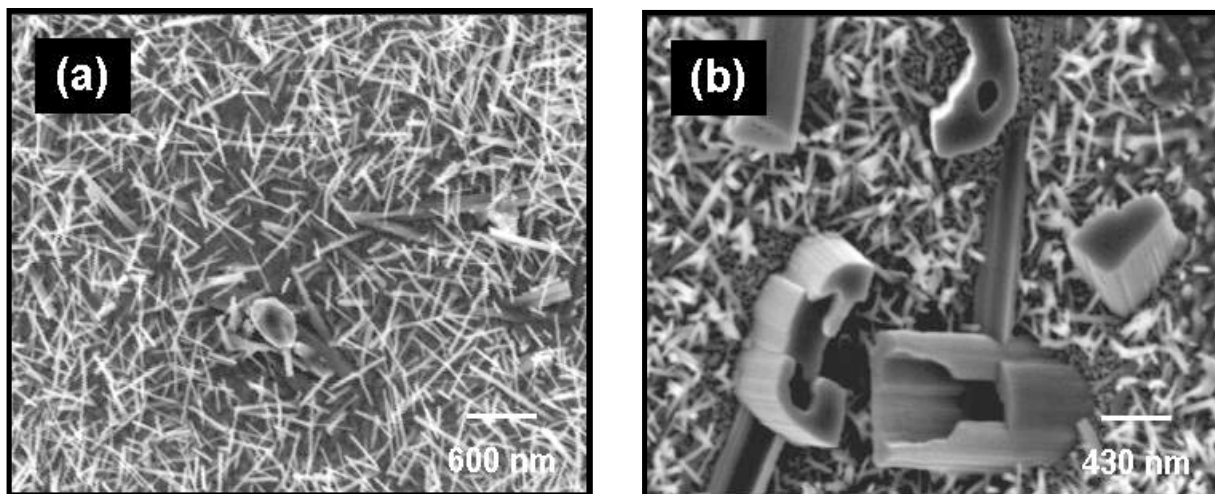


Figure 6. Micrographs of tungsten film surface on heating in CO – (a) nanowires, (b) hollow nanostructures of irregular shapes.

We have done some preliminary tests on the application of these nanowires as gas sensors. Gas sensing properties of WO_3 nanoparticle films have been studied in the recent past, showing excellent sensitivity to H_2S gas and selectivity to other gases.²⁴ In our experiment, nanowires were grown on a microhotplate,^{25,26} annealed in air at 500 °C for 30 minutes, which possibly completely oxidizes them into WO_3 , and then exposed to the test gas (20 ppm of NO_2/NO in air). In comparison with the sensor responses from a bare tungsten coated surface annealed under similar conditions for the same length of time, the nanowire-coated surface was found to be much more sensitive to such low concentrations of NO_x , as seen in Figure 7, and the measurements could be repeated.

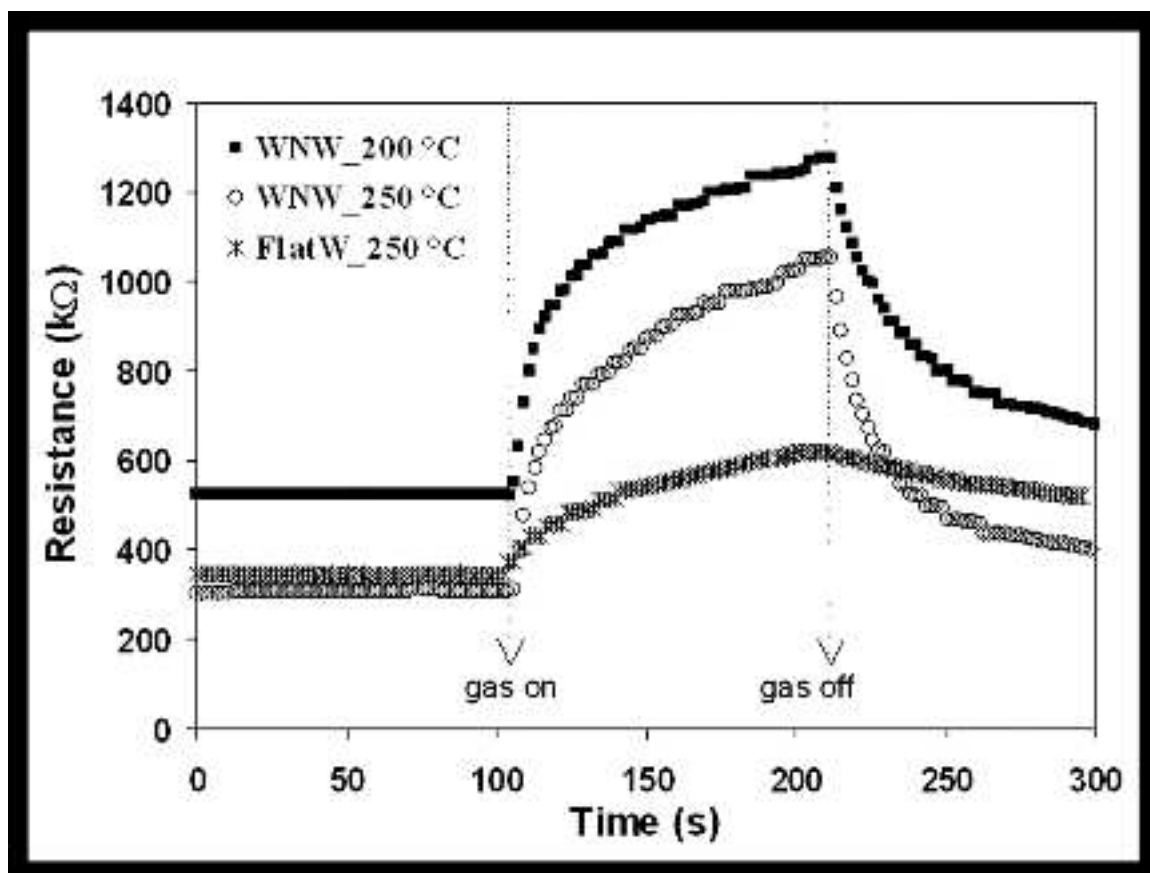


Figure 7. Gas sensor response curves from an annealed nanowire coated surface and an annealed flat tungsten thin film surface, both exposed to 20 ppm of test gas NO_2/NO .

In summary, we have developed a method of restructuring tungsten substrates into tungsten oxide nanowires and hollow microducts by simple thermal treatment in RF plasma at temperatures in the range of 550-620 °C, in the presence of a reducing gas like H_2 or CO . The nanowires have diameters between 10-30 nm and lengths up to 500 nm while the microducts have square edge lengths of approximately 0.5 μm and lengths up to a few hundred μm 's. It is worth pointing out that the growth temperature of tungsten oxide nanowires in our work is significantly lower (by about 250 °C) than previous methods. A trace amount of background oxygen is essential in growth of these nanostructures, which can be grown preferentially by controlling the mass transfer rate of gas phase species to various regions on the substrate. Nanowires were also grown on commercial tungsten wires and tungsten coated TEM grids, indicating the generality of the process. Apart from field emission sources,⁹ these nanowires could be employed as tips for STM and AFM. In addition, nanowires annealed in air are capable of sensing low concentrations of NO_x . The hollow microducts could find applications as building blocks for many functional devices like micro-batteries, as micro-fluidic channels, and in micro-encapsulation for drug delivery.¹⁶

REFERENCES

1. (a) Y. Xia, P. Yang, Y. Sun, Y. Wu, B. Mayers, B. Gates, Y. Yin, F. Kim, H. Yan: One-dimensional nanostructures: Synthesis, characterization and applications. *Adv. Mater.*, **15**, 353 (2003).
2. C.N.R. Rao, F.L. Deepak, G. Gundiah, A. Govindaraj: Inorganic nanowires. *Progress in Solid State Chemistry*, **31**, 5 (2003).
3. S. Iijima: Helical microtubules of graphitic carbon. *Nature*, **354**, 56 (1991).
4. Robert C. Haddon, (ed.), Special issue on carbon nanotubes. *Acc. Chem. Res.*, **36**, 997 (2002).
5. Z.W. Pan, Z.R. Dai, Z.L. Wang: Nanobelts of semiconducting oxides. *Science*, **291**, 1947 (2001).
6. S. Matsui, Y. Ochiai: Focused ion beam applications to solid state devices. *Nanotechnology*, **7**, 247 (1996).
7. B. Gates, B. Mayers, B. Cattle, Y. Xia: Novel nanostructures of functional oxides synthesized by thermal evaporation. *Adv. Funct. Mater.*, **12**, 219 (2002).
8. Y. Zhang, N. Wang, S. Gao, R. He, S. Miao, J. Liu, J. Zhu, X. Zhang: A simple method to synthesize nanowires. *Chem. Mater.*, **14**, 3564 (2002).
9. J.C. Hulteen, C.R. Martin: A general template-based method for the preparation of nanomaterials. *J. Mater. Chem.*, **7**, 1075 (1997).
10. C. Mu, Y. Yu, R. Wang, K. Wu, D. Xu, G. Guo: Uniform metal nanotube arrays by multistep template replication and electrodeposition. *Adv. Mater.*, **16**, 1550 (2004).
11. E.C. Walter, K. Ng, M.P. Zach, R.M. Penner, F. Favier: Electronic devices from electrodeposited metal nanowires. *Microelectron. Engg.*, **61-62**, 555 (2002).
12. E. Tosatti, S. Prestipino: Weird gold nanowires. *Science*, **289**, 561 (2000).
13. Y.H. Lee, C.H. Choi, Y.T. Jang, E.K. Kim, B.K. Ju, N.K. Min, J.H. Ahn: Tungsten nanowires and their field electron emission properties. *Appl. Phys. Letters*, **81**, 745 (2002).
14. G. Gu, B. Zheng, W.Q. Han, S. Roth, J. Liu: Tungsten oxide nanowires on tungsten substrates. *Nano Letters*, **2**, 849 (2002).
15. J. Zhou, N.S. Xu, S.Z. Deng, J. Chen, J.C. She, Z.L. Wang: Large area nanowire arrays of

- molybdenum and molybdenum oxides: Synthesis and field emission properties. *Adv. Mater.*, **15**, 1835 (2003).
16. J. Liu, Y. Zhao, Z. Zhang: Low-temperature synthesis of large-scale arrays of aligned tungsten oxide nanorods. *J. Phys. Cond. Matter.*, **15**, 453 (2003).
17. S. Vaddiraju, H. Chandrasekaran, M. Sunkara: Vapor phase synthesis of tungsten nanowires. *J. Am. Chem. Soc.*, **125**, 10792 (2003).
18. F. Okuyama: Crystalline tungsten grown by reducing vapor-deposited tungsten oxide. *J. Cryst. Growth*, **38**, 103 (1977).
19. D. Veblen, J. Post: A TEM study of fibrous cuprite (chalcotrichite): microstructures and growth mechanisms. *American Mineralogist*, **68**, 790 (1983).
20. V.K. Sarin: Morphological changes occurring during the reduction of WO_3 . *J. Mater. Sci.*, **10**, 593 (1975).
21. W.B. Hu, Y.Q. Zhu, W.K. Hsu, B.H. Chang, M. Terrones, N. Grobert, H. Terrones, J.P. Hare, H.W. Kroto, D.R.M. Walton: Generation of hollow crystalline tungsten oxide fibers. *Appl. Phys. A*, **70**, 231 (2000).
22. Y. Li, Y. Bando, D. Goldberg: Quasi-aligned single-crystalline $\text{W}_{18}\text{O}_{49}$ nanotubes and nanowires. *Adv. Mater.*, **15**, 1294 (2003).
23. B. Mayers, Y. Xia: Formation of tellurium nanotubes through concentration depletion at the surface of seeds. *Adv. Mater.*, **14**, 279 (2002).
24. J.L. Solis, A. Hoel, L.B. Kish, S. Sauko, V. Lantto, C.G. Granqvist: Gas sensing properties of nanocrystalline WO_3 films made by advanced reactive gas deposition. *J. Am. Ceram. Soc.*, **84**, 1504 (2001).
25. J.S. Suehle, R.E. Cavicchi, M. Gaitan, S. Semancik: Tin oxide gas sensor fabricated using CMOS microhotplates and in-situ processing. *IEEE Electron Device Letters*, **14**, 118 (1993).
26. R.E. Cavicchi, S. Semancik, F. DiMeo Jr., C.J. Taylor: Use of microhotplates in the controlled growth and characterization of metal oxides for chemical sensing. *J. Electroceramics*, **9**, 155 (2002).

